Research Square

Preprints are preliminary reports that have not undergone peer review.
They should not be considered conclusive, used to inform clinical practice,
or referenced by the media as validated information.

Are MoCA subdomains deficits linked to white matter changes in early Huntington's disease? A diffusion MRI approach

Esquiliano Ricardo
Universidad Panamericana
Cancino-Pérez Valeria
Universidad Panamericana
Fernandez-Ruiz Juan
Universidad Nacional Autónoma de México
Blanco-Cortes Milka
University of Toronto
Galvez Victor
vgalvez@up.edu.mx
Universidad Panamericana

Research Article

Keywords: Huntington's Disease, MoCA, Visuospatial, White Matter, fMRI, Fractional Anisotropy, Mean diffusivity, TBSS

Posted Date: April 9th, 2026

DOI: https://doi.org/10.21203/rs.3.rs-8971620/v1

License: This work is licensed under a Creative Commons Attribution 4.0 International License.
Read Full License

Additional Declarations: No competing interests reported.

Abstract

This study explored the relationship between the Montreal Cognitive Assessment's (MoCA) subdomains and white matter changes in Huntington's disease (HD). Fractional anisotropy (FA) and mean diffusivity (MD) were measured using Diffusion Tensor Imaging (DTI) in 22 early manifest HD patients and 20 healthy controls. Tract-Based Spatial Statistics was used to compare the two groups and correlate patients' FA and MD values with their performance in MoCA subdomains. Among all MoCA subdomains, only visuospatial performance was associated with white matter integrity in the corpus callosum, corona radiata, and superior longitudinal fasciculus, supporting the feasibility of combining DTI analysis with screening tools to monitor non-motor symptoms.

Introduction

Huntington's disease (HD) is a genetic neurodegenerative disorder characterized by neuropsychiatric, cognitive, and motor symptoms, typically manifesting in early adulthood (Philips et al., 2013). Cognitive impairment becomes prominent as the disease progresses, especially affecting executive functions and visuospatial performance (Migliore et al., 2021; Hart et al., 2013). Although cognitive deterioration is a characteristic non-motor symptom of HD, premanifest and manifest patients exhibit different features of decline (Del Pino et al., 2025).

While basal ganglia degeneration is the hallmark of HD neuro-pathophysiology (Liu et al., 2023), early changes in white matter (WM) also play a critical role. These changes result from the breakdown of myelinated fibers and axonal degeneration, particularly in the prefrontal tracts, corpus callosum (CC), and corticospinal tracts (Bourbon-Teles et al., 2019; Estevez-Fraga et al., 2020). Magnetic resonance imaging (MRI) studies have correlated executive functions with WM changes in patients, quantifying diffusion tensor imaging (DTI) parameters, such as fractional anisotropy (FA) and mean diffusivity (MD) (Bohanna et al., 2011). However, cognitive deficits are often detected using extensive neuropsychological batteries, which are time-consuming and require highly trained personnel (Gluhm et al., 2013; Rosca & Simu, 2020).

As an alternative, the Montreal Cognitive Assessment (MoCA) has emerged as a brief, easy-to-administer tool for detecting mild cognitive impairment (MCI; MoCA score < 26/30) in HD patients (Gluhm et al., 2013; Nasreddine et al., 2005). Furthermore, MoCA assesses a broad range of cognitive subdomains, facilitating research into functional and structural brain deterioration (Videnovic et al., 2010). For example, fMRI studies in HD patients have shown a correlation between language subdomain scores and cortical thinning in regions such as the lingual and fusiform gyri, supramarginal gyrus, and lateral orbitofrontal lobe (Sweidan et al., 2020). Despite these findings, the relationship between MoCA-assessed cognitive subdomains and WM changes in HD remains unclear.

This study aims to explore the link between cognitive deficits and WM differences in early manifest HD by correlating MoCA subdomain scores with DTI parameters. The hypothesis is that low performance on MoCA subdomains is associated with interhemispheric and prefrontal WM changes in patients.

Methods

Participants

Twenty-two patients with a molecular diagnosis of HD and 20 age-matched healthy controls participated in the study (Table 1). Patients were recruited at the National Institute of Neurology and Neurosurgery (INNN) in Mexico City. MoCA scores were grouped into five cognitive subdomains: attention/executive (digit span, target detection, serial seven subtraction, Trail Making Test B, fluency, and abstraction), visuospatial (clock drawing and three-dimensional cube copying), language (object naming and sentence repetition), memory (recall of five previously presented words), and orientation (temporal and spatial) (Gluhm et al., 2013).

Image Acquisition

All images were acquired using a 3T MRI scanner from Philips Medical Systems in Eindhoven, The Netherlands. The high-resolution anatomical images were obtained using a T1-3D Fast Field Echo sequence with the following parameters: TR/TE of 8/3.7 ms, a field of view (FOV) of 256 × 256 mm^2, a flip angle of 8°, an acquisition and reconstruction matrix of 256 × 256, and an isometric resolution of 1 × 1 × 1 mm^3. The DTI sequences were conducted using Single-Shot Echo Planar Imaging. This involved acquiring 33 volumes of 70 axial slices (with a slice thickness of 2 mm and no separation), corresponding to each of the 32 independent diffusion directions with a b-value of 800 s/mm^2, along with one volume for b = 0 s/mm^2. The DTI sequence parameters included a TR/TE of 8467/60 ms, a FOV of 256 × 256 mm^2, and an acquisition and reconstruction matrix of 128 × 128, resulting in an isometric resolution of 2 × 2 × 2 mm^3.

Diffusion Tensor Analysis

The DTI images were processed using the FSL Diffusion toolbox (Smith et al., 2007). First, the effects of eddy currents were corrected, and the diffusion tensor model was adjusted to generate FA and MD maps for each participant. Subsequently, statistical analysis was performed using the Tract-Based Spatial Statistics (TBSS) approach, following: 1) identification of a common registration target and alignment of all participants' FA images to this target; 2) creation of a mean FA map using the mean of all aligned FA images and of a thresholded skeletonized mean FA image (threshold = 0.2); 3) and projection of each participant's FA image onto the skeleton and voxel-wise statistical analysis across subjects on the skeleton-space FA data; 4) Using the same nonlinear registration, derived from the FA analysis, MD data were projected onto the skeleton vectors before voxel-wise statistical analysis across subjects (Smith et al., 2007, Smith et al., 2004).

Statistical comparison of the groups

A two-sample t-test was conducted using FSL's *randomise* function to compare the patient and healthy groups, controlling for age. To address multiple comparisons, we applied the Threshold-Free Cluster Enhancement (TFCE) method (Winkler et al., 2014). Only voxels that survived family-wise error correction (FWE) with $p < 0.05$ were considered significant between the two groups. The final parametric maps were parcellated, binarized, and labeled using the WM atlas developed at Johns Hopkins University.

Cognitive correlations of WM with MoCA and its subdomains

The associations between WM density and the cognitive deficits in patients with HD were examined using analysis of covariance (ANCOVA) by TBSS. Six different analyses were run. In the first analysis, FSL *randomise* was fed with the total MoCA scores. The subsequent analyses used the scores of each cognitive subdomain. To correct for multiple comparisons, randomized permutations were employed using the TFCE method (Winkler et al., 2014). Only voxels that survived FWE correction with $p < 0.05$ were considered statistically significant. In all analyses, the disease burden score (calculated as age (years) × (CAG repeat length − 35.5)) was included as a nuisance variable (Poudel et al., 2014).

Subsequently, the FA and MD peak values in the significant voxels were selected for each patient. As the cognitive measurements did not follow a normal distribution, as determined by the Shapiro-Wilk test ($p < 0.05$), Spearman correlations were conducted between the diffusion measurements with the MoCA score and its five cognitive subdomains. Significant correlations were defined as those with p-values less than 0.05.

Multiple linear regression analyses between diffusion and gray matter

To dissociate the role of volumetric changes in gray matter from those in WM, a multiple linear regression was conducted to assess the combined subcortical effects on cognitive performance. Volumetric data were obtained from T1-3D images of patients using the volBrain pipeline (https://www.volbrain.net/home) (Coupé et al., 2020). Statistical analyses were conducted in RStudio version 3.6.0.

Ethical and Data Availability Statement

The study was approved by the INNN's Research and Ethics Committee (N' DIC/419/14 and N' 41/14). All participants provided written informed consent, as outlined in the Declaration of Helsinki (World Medical Association, 2024).

Results

Demographic and clinical data

Controls and patients were matched for age (U = 198.5), area of residence, and education level (U = 275). The volunteers included in the control group had no history of neurological injury or psychiatric diseases reported by clinical interview (Table 1). The TFC scale mean score for HD subjects was 11.8 ± 1.8, detecting 17 patients (77%) in Stage I (scores 11–13) and 5 patients (22.7%) in Stage II (scores 7–10). The mean UHDRS score was 14.6 ± 10.6 out of a maximum of 124. One patient (4.5%) showed abnormal movements, with the most affected patient scoring 40 points. Seventeen patients (77.3%) scored less than 17 points, and two patients (9.5%) scored 0 points. The above data confirmed their early clinical status, as reflected in functional and motor decline (Schobel et al., 2017).

Table 1
Clinical data

Male-to-female ratio	**Control healthy group** ***mean ± standard deviation (range)***	**HD group** ***mean ± standard deviation (range)***
	9:11	**9:13**
Age in years	45.8 ± 11.9 (26.5–67.5)	46.1 ± 12.1 (27.6–67.7)
Education in years	16.6 ± 2.8 (9–22)	14.1 ± 3.2 (9–19)
Age onset in years		48.8 ± 11.5 (28–70)
Symptoms Duration in months		59.5 ± 53.4 (0-137.36)
CAG-Repeat Length		44.5 ± 3.8 (40–54)
Disease Burden		385.6 ± 100.3 (153-536.5)
UHDRS motor scale		14.6 ± 10.6 (0–40)
TFC		11.8 ± 1.8 (8–13)

Diseased Burden: Age (years) × (CAG-repeat length − 35.5). To classify patients with early-onset Huntington's disease, symptomatic HD individuals were identified based on their Total Functional Capacity (TFC) scores, with lower values indicating reduced functional capacity. TFC assessment, ranging from 0 to 13 (early symptomatic HD > 7), and the UHDRS (Unified Huntington's Disease Rating Scale) were used to assess disease severity. A single outlier pushed the UHDRS range to 40.

MoCA performance

MoCA performance in HD patients (median = 24; U = 344.5, p < .05) was statistically lower than that of the control group (median = 28). In addition, the HD group obtained low scores in the following MoCA subdomains: language (median = 4; U = 294, p < .03), attention/executive (median = 8; U = 342, p < .05), and visuospatial (median = 4; U = 296, p < .01) (Fig. 1).

WM changes in HD patients

TBSS group comparison revealed significantly lower FA values (Fig. 2a) in patients' right/left external capsules, the body of the corpus callosum (BCC), and the posterior/anterior right corona radiata. Conversely, there were significantly high MD values (Fig. 2b), mainly in the right superior longitudinal fasciculus (SLF), the right superior corona radiata (SCR), and the splenium of the corpus callosum (Supplementary Table 1).

MoCA subdomain performance and its correlation with WM changes in HD patients

Although patients exhibited lower language and attention/executive performance than the control group, no significant relationship was found between their scores and WM integrity ($p = .48$ and $p = .09$, respectively). Nonetheless, the visuospatial subdomain was the only one correlated with DTI parameters in the HD group. As performance increased, the higher voxel peak FA were identified in the BCC, left SLF, and left SCR (Fig. 3a). Additionally, a negative correlation was observed between the higher voxel-peak MD and visuospatial scores in the BCC, right SLF, and left SCR (Fig. 3b). Although other WM regions were also identified (Table 2), the subsequent analysis used the higher FA and MD voxel peak values along with visuospatial scores.

Table 2
Visuospatial correlation with FA and MD

FA Correlations					
Anatomical Regions	MNI Coordinates			r	*p* <
	x	y	z		
Body of the corpus callosum	-10	-22	27	.80	.001
Left superior longitudinal fasciculus	-42	-47	33	.83	.001
Left superior corona radiata	-19	-23	38	.71	.001
Inferior fronto-occipital fasciculus	28	-54	19	.81	.001
Right arcuate fasciculus	38	-37	18	.76	.001
Left uncinate fasciculus	-23	9	-13	.78	.001
Forceps minor	11	28	-7	.78	.001
Right anterior thalamic radiation	22	32	15	.76	.001
Left external capsule	-32	-11	8	.74	.001
MD Correlations					
Anatomical Regions	MNI Coordinates			r	*p* <
	x	y	z		
Body of the corpus callosum	-13	-30	27	− .88	.001
Right superior longitudinal fasciculus	49	-33	37	− .86	.001
Left superior corona radiata	-22	-16	37	− .79	.005
Forceps minor	10	31	8	− .79	.001
Left dorsal cingulum subsection	-11	-35	31	− .94	.001
Right dorsal cingulum subsection	8	-23	36	− .90	.001
Left posterior limb of the internal capsule	-21	-4	15	− .73	.001
Right inferior fronto-occipital fasciculus	40	35	1	− .69	.008
Right posterior corona radiata	25	-24	23	− .75	.001
Left anterior limb of the internal capsule	-19	11	12	− .76	.001

All correlations were performed using Spearman's rank correlation, with p < .05 considered significant. FA, Fractional Anisotropy; MD, Mean Diffusivity; MNI, Montreal Neurological Institute 152 Atlas.

Correlation between MoCA scores and subcortical brain structures

A moderate correlation was found between MoCA scores and the volumes of the left ($r = 0.46$; $p < .03$) and right ($r = 0.44$; $p < .04$) caudate. All other subcortical structures did not meet the significant correlations of $p < .05$.

Multiple linear regression analyses between diffusion and gray matter

The linear regression models were conducted using FA and MD values from visuospatially relevant tracts: BCC, SLF, and SCR, as dependent variables. Ventricular and caudate nucleus volumes were entered simultaneously as predictors to assess whether their changes served as strong predictors of the previously observed diffusion associations.

A significant association was found between right ventricular volume and BCC integrity ($\beta = -0.01$, $p < .04$). No significant effects were observed for ventricular volumes in the SLF or SCR, nor for caudate nucleus volumes in any tract. A significant association was found between right ventricular volume and BCC integrity ($\beta = -0.01$, $p < .04$). No significant effects were observed for ventricular volumes in the SLF or SCR, nor for caudate nucleus volumes over any tract (Supplementary Table 2).

The volumetric list, including all regions of interest (ROIs), is available at: https://doi.org/10.6084/m9.figshare.27893361.v2.

Discussion

This study aimed to explore the link between cognitive deficits and WM differences in early HD by correlating MoCA subdomain scores with diffusion parameters. The first TBSS analysis identified the main WM changes in HD patients. The second analysis explored the correlation between scores on all MoCA subdomains and WM changes in the patients. The main finding was a significant relationship between visuospatial scores and the integrity of the BCC, SLF, and SCR.

Cognitive deficits in HD are primarily driven by early WM pathophysiology. Patients exhibited lower overall performance on the global MoCA and reduced WM integrity compared to the control group. The structural changes observed in the BCC and CR tracts, which are heavily connected to cortical and subcortical areas, align with findings from other studies showing a pattern of degeneration that starts in deep brain regions of patients with HD (Della Nave et al., 2010). Therefore, these WM alterations reduce the efficiency of signal transmission between brain regions, affecting both motor and cognitive functions from the early stages of HD (Rosas et al., 2018), as shown in studies using the MoCA to assess patients' status (Rosca & Simu, 2020).

Visuospatial deficits in HD patients are linked to WM disruption in communication pathways between motor and perceptual brain areas. The patients' SLF, CR, and BCC integrity were the primary effects associated with low MoCA visuospatial scores. These results are followed by a previous report that describes SLF and CR changes in HD patients (Della Nave et al., 2010). Particularly, the CR is involved in motor planning, cognitive flexibility, and processing speed (Yu et al., 2022). Similarly, SLF is a crucial component of the visuospatial attentional network, since it connects the frontal lobe with the parietal cortex (Bernard et al., 2020). This network processes and integrates visual and spatial information, facilitating orientation, attention allocation, visual search, hand-eye coordination, object recognition, and spatial memory (Kargar & Jalilan, 2024). Also, the BCC contributes significantly to precise motor control, including real-time adjustments based on perceptual feedback (Phillips et al., 2013; Bohana et al., 2011). Therefore, changes in BCC, SLF, and CR would impair performance in copying and drawing tasks, typically observed in the early HD stages (Dridan et al., 2012; Johnson et al., 2015).

Visuospatial deficits in HD patients are also driven by reduced interhemispheric connectivity. The MoCA visuospatial subdomain correlated with the BCC integrity. Despite the regression analysis suggesting that ventricular enlargement, a common neuroanatomical hallmark of HD, may partially contribute to alterations in BCC diffusion, the absence of significant ventricular effects on the SLF and SCR, together with the lack of associations between caudate nucleus volumes and across all examined tracts, suggests that ventricular expansion alone does not fully account for the visuospatial deficits. It is important to highlight that the BCC alteration is associated with decreased pyramidal cells, as its fibers originate from these neurons, which are affected from the manifest to advanced stages of the illness (Blumenstock & Dudanova, 2020). Then, interhemispheric disruption could hinder the coordination of motor and perceptual abilities required for visuospatial performance as observed in manifest HD patients (Coppen et al., 2019).

MoCA’s visuospatial component can be used to track brain changes in HD. Although brief, the visuospatial tasks were a feasible measure that enabled the detection of correlations between FA and MD values and neuroanatomical changes. Previous studies support the notion that this skill is among the earliest cognitive deficits in HD, making the findings coherent (Labuschagne et al., 2016). However, some studies have struggled to find a correlation between MoCA visuospatial tasks and brain changes (Sweidan et al., 2020; Poudel et al., 2014), possibly because they overlooked the proposed arrangement of MoCA’s subdomains, specifically for HD patients (Gluhm et al., 2013).

The limitations of the present study to be addressed in future designs were: 1) conducting cognitive follow-up to observe participants' progress, and 2) further addressing fiber bundle overlap by using techniques such as Fixel-Based Analysis, which can differentiate between fiber bundles within a voxel (Raffelt et al., 2015).

Conclusion

The visuospatial deficits identified by the MoCA were associated with the main WM regions affected in early manifest HD, specifically the SLF, BCC, and CR. The above supports the advantages of combining DTI analysis with cognitive screening tools in HD research on non-motor symptoms.

Declarations

Author Contribution

E. R contributed on the main writing of the paper, as well as the statistical analysis of the fMRI images CP. V writing riview and editing, running statistical analysisFR. J revision of the statistical analysys, disigner of the study BC.M review and editing of the manuscript G.V conceptualization of the study , approval and supervition of the study, funding acquisition and review and revition of the manuscript

Declaration of Conflicting Interest

The authors declare no potential conflicts of interest concerning this article.

Funding Declaration

This research was funded by "Fondo de apoyo a la Investigación de la Facultad de Ciencias de la Salud - Universidad Panamericana" CIP-PI-115-3, granted to Victor Galvez, for the period 2025–2027.

Human Ethics and Consent to Participate declarations

We confirm that all participants have provided written informed consent. The Ethical Committee from the National Neurology Institute approved the informed consent letter (N’ 41/14).

Clinical trial number: not applicable

References

1. Bernard, F., Lemée, J., Mazerand, E., Leiber, L., Menei, P., & Minassian, T., A (2020). The ventral attention network: The mirror of the language network in the right brain hemisphere. *Journal of Anatomy*, *237*(4), 632–642. https://doi.org/10.1111/joa.13223
2. Blumenstock, S., & Dudanova, I. (2020). Cortical and striatal circuits in Huntington’s disease. *Frontiers in Neuroscience*, *14*, 82. https://doi.org/10.3389/fnins.2020.00082
3. Bohanna, I., Georgiou-Karistianis, N., Sritharan, A., Asadi, H., Johnston, L., Churchyard, A., & Egan, G. (2011). Diffusion tensor imaging in Huntington’s disease reveals distinct patterns of white matter degeneration associated with motor and cognitive deficits. *Brain Imaging and Behavior*, *5*(3), 171–180. https://doi.org/10.1007/s11682-011-9121-8
4. Bourbon-Teles, J., Bells, S., Jones, D. K., Coulthard, E., Rosser, A., & Metzler-Baddeley, C. (2019). Myelin breakdown in human Huntington’s disease: Multimodal evidence from diffusion MRI and

quantitative magnetization transfer. *Neuroscience*, *403*, 79–92. https://doi.org/10.1016/j.neuroscience.2017.05.042

5. Coppen, E. M., Jacobs, M., van der Zwaan, K. F., Middelkoop, H. A. M., & Roos, R. A. C. (2019). Visual object perception in premanifest and early manifest Huntington's disease. *Archives of Clinical Neuropsychology*, *34*(8), 1320–1328. https://doi.org/10.1093/arclin/acz002
6. Coupé, P., Mansencal, B., Clément, M., Giraud, R., de Senneville, B. D., Ta, V. T., et al. (2020). AssemblyNet: A large ensemble of CNNs for 3D whole brain MRI segmentation. *Neuroimage*, *219*, 117026. https://doi.org/10.1016/j.neuroimage.2020.117026
7. Del Pino, R. D., Acera, M. Á., de Ortiz, A. O., Tijero, B., Ruiz-López, M., Somme, J., et al. (2025). Characterization of visual cognition in pre-manifest, manifest, and reduced penetrance Huntington's disease. *Scientific Reports*, *15*(1), 4707. https://doi.org/10.1038/s41598-025-88406-5
8. Della Nave, R., Ginestroni, A., Tessa, C., Giannelli, M., Piacentini, S., Filippi, M., et al. (2010). Regional distribution and clinical correlates of white matter structural damage in Huntington disease: A tract-based spatial statistics study. *American Journal of Neuroradiology*, *31*, 1675–1681. https://doi.org/10.3174/ajnr.A2128
9. Dridan, B. A., Ong, B., Lloyd, S., Evans, L., & Crowe, S. F. (2013). The simple copy task: Detecting higher order visual processing deficits in schizophrenia, dementia, and movement disorder groups. *Australian Psychologist*, *48*(2), 98–109. https://doi.org/10.1111/j.1742-9544.2012.00067.x
10. Estevez-Fraga, C., Scahill, R., Rees, G., Tabrizi, S. J., & Gregory, S. (2021). Diffusion imaging in Huntington's disease: A comprehensive review. *Journal of Neurology Neurosurgery & Psychiatry*, *92*(1), 62–69. https://doi.org/10.1136/jnnp-2020-324377
11. Gluhm, S., Goldstein, J., Brown, D., Van Liew, C., Gilbert, P. E., & Corey-Bloom, J. (2013). Usefulness of the Montreal Cognitive Assessment (MoCA) in Huntington's disease. *Movement Disorders*, *28*(12), 1744–1747. https://doi.org/10.1002/mds.25578
12. Hart, E. P., Dumas, E. M., Giltay, E. J., Middelkoop, H. A. M., & Roos, R. A. C. (2013). Cognition in Huntington's disease in manifest, premanifest, and converting gene carriers over ten years. *Journal of Huntington's Disease*, *2*(2), 137–147. https://doi.org/10.3233/JHD-130059
13. Johnson, E. B., Rees, E. M., Labuschagne, I., Durr, A., Leavitt, B. R., Roos, R. A. C., et al. (2015). The impact of occipital lobe cortical thickness on cognitive task performance: An investigation in Huntington's disease. *Neuropsychologia*, *79*, 138–146. https://doi.org/10.1016/j.neuropsychologia.2015.10.033
14. Kargar, Y., & Jalilian, M. (2024). Anatomo-functional profile of white matter tracts in relevance to language: A systematic review. *Journal of Neurolinguistics*, *69*, 101175. https://doi.org/10.1016/j.jneuroling.2023.101175
15. Labuschagne, I., Cassidy, A. M., Scahill, R. I., Johnson, E. B., Rees, E., O'Regan, A., et al. (2016). Visuospatial processing deficits linked to posterior brain regions in premanifest and early stage Huntington's disease. *Journal of the International Neuropsychological Society*, *22*(6), 595–608. https://doi.org/10.1017/S1355617716000321

16. Liu, C. F., Younes, L., Tong, X. J., Hinkle, J. T., Wang, M., Phatak, S., et al. (2023). Longitudinal imaging highlights preferential basal ganglia circuit atrophy in Huntington's disease. *Brain Communications*, *5*(5), fcad214. https://doi.org/10.1093/braincomms/fcad214
17. Migliore, S., D'Aurizio, G., Maffi, S., Ceccarelli, C., Ristori, G., Romano, S., et al. (2021). Cognitive and behavioral associated changes in manifest Huntington disease: A retrospective cross-sectional study. *Brain and Behavior*, *11*(7), e02151. https://doi.org/10.1002/brb3.2151
18. Nasreddine, Z. S., Phillips, N. A., Bédirian, V., Charbonneau, S., Whitehead, V., Collin, I., & Chertkow, H. (2005). The Montreal Cognitive Assessment, MoCA: A brief screening tool for mild cognitive impairment. *Journal of the American Geriatrics Society*, *53*(4), 695–699. https://doi.org/10.1111/j.1532-5415.2005.53221.x
19. Phillips, O., Sanchez-Castaneda, C., Elifani, F., Maglione, V., Di Pardo, A., Caltagirone, C., Squitieri, F., Sabatini, U., & Di Paola, M. (2013). Tractography of the corpus callosum in Huntington's disease. *PLOS ONE*, *8*(9), e73280. https://doi.org/10.1371/journal.pone.0073280
20. Poudel, G. R., Stout, J. C., Domínguez, D. J. F., Churchyard, A., Chua, P., Egan, G. F., et al. (2014). Longitudinal change in white matter microstructure in Huntington's disease: The IMAGE-HD study. *Neurobiology of Disease*, *74*, 406–412. https://doi.org/10.1016/j.nbd.2014.12.009
21. Raffelt, D. A., Smith, R. E., Ridgway, G. R., Tournier, J. D., Vaughan, D. N., Rose, S., et al. (2015). Connectivity-based fixel enhancement: Whole-brain statistical analysis of diffusion MRI measures in the presence of crossing fibres. *Neuroimage*, *117*, 40–55. https://doi.org/10.1016/j.neuroimage.2015.05.039
22. Roșca, E. C., & Simu, M. (2020). Montreal Cognitive Assessment for evaluating cognitive impairment in Huntington's disease: A systematic review. *CNS Spectrums*, *27*(1), 27–45. https://doi.org/10.1017/S1092852920001868
23. Rosas, H. D., Wilkens, P., Salat, D. H., Mercaldo, N. D., Vangel, M., Yendiki, A. Y., et al. (2018). Complex spatial and temporally defined myelin and axonal degeneration in Huntington disease. *NeuroImage: Clinical*, *20*, 236–242. https://doi.org/10.1016/j.nicl.2018.01.029
24. Schobel, S. A., Palermo, G., Auinger, P., Long, J. D., Ma, S., Khwaja, O. S., et al. (2017). Motor, cognitive, and functional declines contribute to a single progressive factor in early Huntington's disease. *Neurology*, *89*(24), 2495–2502. https://doi.org/10.1212/WNL.0000000000004743
25. Smith, S. M., Jenkinson, M., Woolrich, M. W., Beckmann, C. F., Behrens, T. E. J., Johansen-Berg, H. (2004). Advances in functional and structural MR image analysis and implementation as FSL. *NeuroImage, 23*(Suppl. 1), S208–S219. https://doi.org/10.1016/j.neuroimage.2004.07.051
26. Smith, S. M., Johansen-Berg, H., Jenkinson, M., Rueckert, D., Nichols, T. E., Miller, K. L., & Behrens, T. E. J. (2007). Acquisition and voxelwise analysis of multi-subject diffusion data with tract-based spatial statistics. *Nature Protocols*, *2*(3), 499–503.
27. Sweidan, W., Bao, F., Bozorgzad, N., & George, E. (2020). White and gray matter abnormalities in manifest Huntington's disease: Cross-sectional and longitudinal analysis. *Journal of Neuroimaging*, *30*(3), 351–358. https://doi.org/10.1111/jon.12699

28. Videnovic, A., Bernard, B., Fan, W., Jaglin, J., Leurgans, S., & Shannon, K. M. (2010). The Montreal Cognitive Assessment as a screening tool for cognitive dysfunction in Huntington's disease. *Movement Disorders*, *25*(3), 401–404. https://doi.org/10.1002/mds.22748
29. Winkler, A. M., Ridgway, G. R., Webster, M. A., Smith, S. M., & Nichols, T. E. (2014). Permutation inference for the general linear model. *Neuroimage*, *92*, 381–397. https://doi.org/10.1016/j.neuroimage.2014.01.060
30. World Medical Association (2024). *WMA Declaration of Helsinki: Ethical principles for medical research involving human participants*. *JAMA*. https://www.wma.net/policies-post/wma-declaration-of-helsinki
31. Yu, Q., Yin, D., Kaiser, M., Xu, G., Guo, M., Liu, F., et al. (2022). Pathway-specific mediation effect between structure, function, and motor impairment after subcortical stroke. *Neurology*, *100*(6). https://doi.org/10.1212/WNL.0000000000201495

Figures

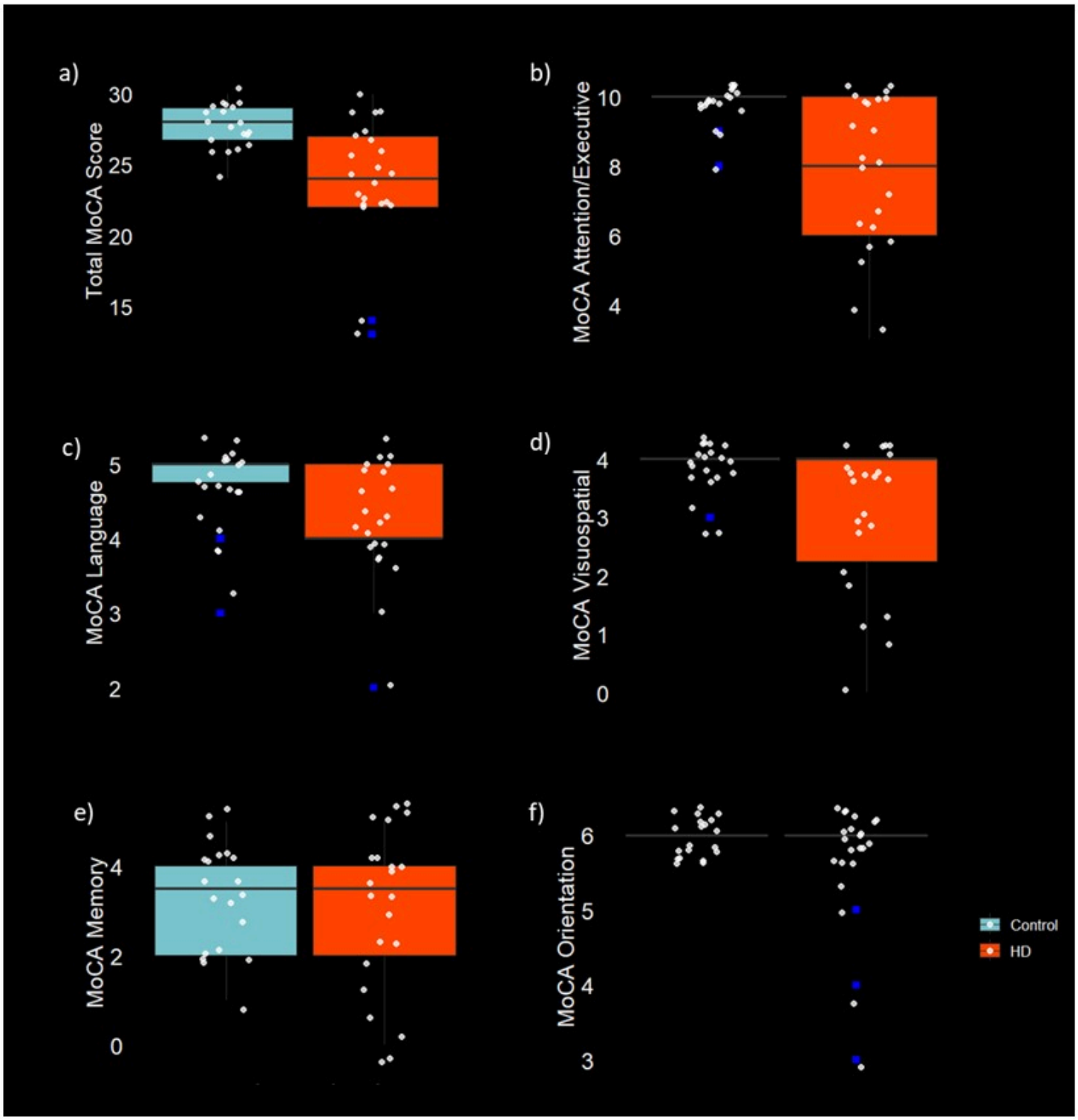

Figure 1

The MoCA global performance and its five cognitive subdomains. Mean scores for each plot were as follows: a) Total MoCA Score: control = 27.6, HD= 24.09; b) MoCA Attention Executive: control = 9.8; HD = 7.8; c) MoCA Language: control = 4.7, HD = 4.2; d) MoCA Visuospatial: control = 3.8, HD = 3.05; e) MoCA Memory: control = 3.3, HD = 3; f)MoCA Orientation: control = 6, HD = 5.6. Blue dots indicate identified outliers. HD: Huntington's Disease.

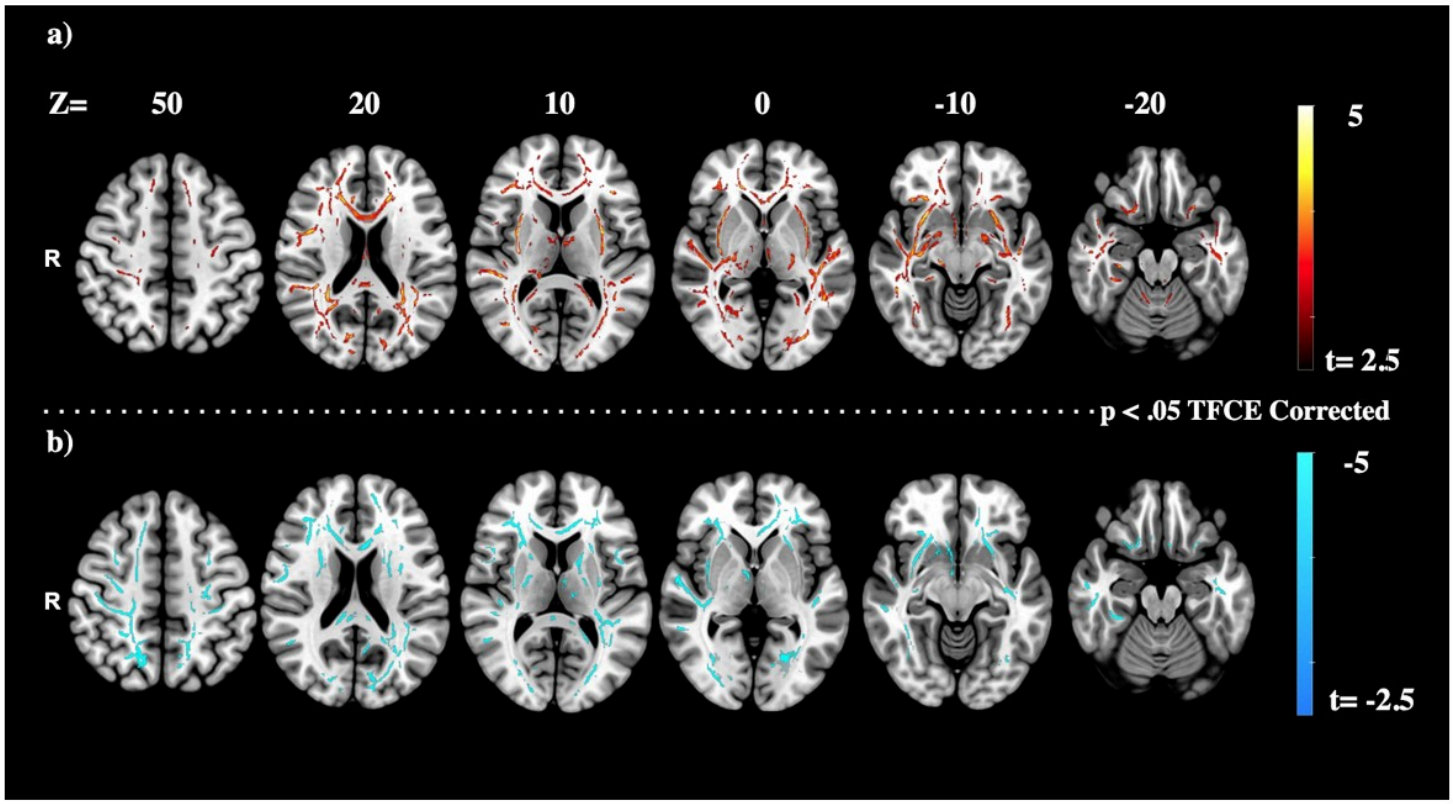

Figure 2

TBSS differences in diffusion parameters between HD and healthy controls. a) Fractional anisotropy decrease in the HD group. b) Mean diffusivity increase in the HD group. TFCE: Threshold-Free Cluster Enhancement method; R: right hemisphere; Z: MNI Atlas Coordinates.

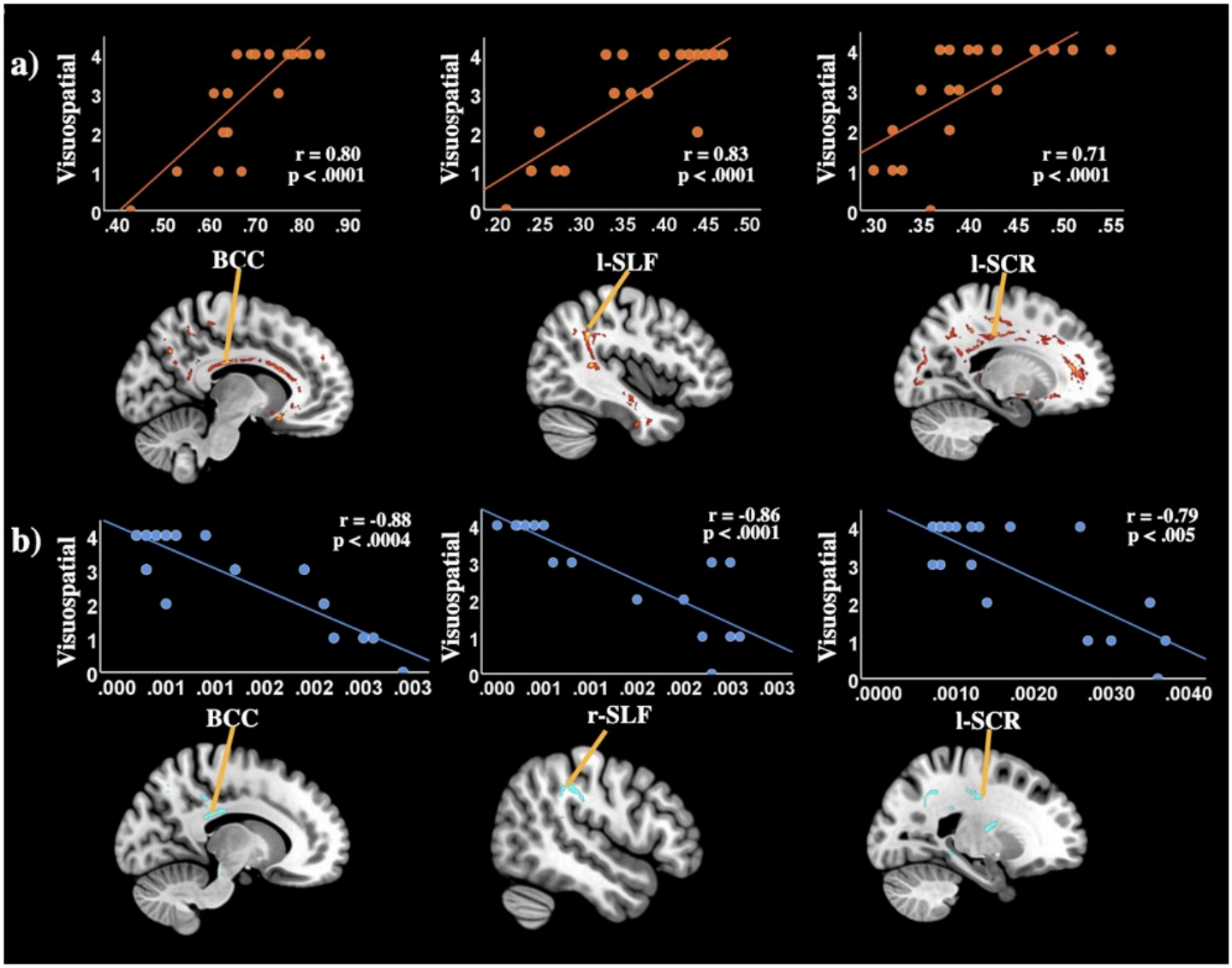

Figure 3

TBSS correlations between diffusion changes and visuospatial MoCA scores. a) Fractional anisotropy. b) Mean diffusivity. BCC: body of corpus callosum; l-SLF: left superior longitudinal fasciculus; l-SCR: left superior corona radiata; r-SLF: right superior longitudinal fasciculus. The scatterplots were generated using the FA and MD voxel's peak values with visuospatial scores.

Supplementary Files

This is a list of supplementary files associated with this preprint. Click to download.

- SupplementaryTables.docx